Journal of Fluids and Structures (1999) **13,** 987–997
Article No.: jfls.1999.0239, available online at http://www.idealibrary.com on IDEAL®

INTERFERENCE EFFECTS FOR A GROUP OF TWO REINFORCED CONCRETE CHIMNEYS

H.-J. Niemann and M. Kasperski

Ruhr-Universität Bochum, Aerodynamik im Bauwesen, 44780 Bochum, Germany

(Received 13 October 1998 and in revised form 11 June 1999)

Based on wind tunnel experiments in a simulated boundary layer flow, interference effects for a group of two 200 m high reinforced concrete chimneys are investigated, in particular the effect of the natural frequencies of the structure on the response. The wind induced forces are measured by a force balance which acts as a mechanical filter. This distortion has to be removed in the frequency domain. For translating the wind tunnel results to full-scale results, the measured signals have to be weighted additionally by the mechanical admittance of the real structure, taking into account the appropriate frequency scale. After correction and weighting in the frequency domain, the signals are re-transferred to the time domain to sample the extremes of the action effects, i.e., the responses, which now include the quasi-static and resonant contribution. To obtain a sufficiently high statistical stability, 60 independent runs are performed for each interference situation. The analysis of the extremes clearly shows that for interference situations the coefficient of variation of the extremes is high. Therefore, an appropriate fractile of the extremes should be used to define the design wind load. This fractile is obtained assuming a Gumbel distribution for the probability distribution of the extreme action effects. Additionally, an appropriate time scale has to be taken into account. The difference between the proposed fractile and the often applied mean value of the extremes is large, with differences up to 20%. Interference leads to a mixed excitation. Besides resonance due to the turbulence of the oncoming flow, considerable resonant excitation may occur due to wake buffeting. While in the first case a lower value of the natural frequency leads to larger action effects, resonance effects due to wake buffeting become worse for a higher value of the natural frequency. Since in the design calculations the natural frequency can be estimated only within a remaining uncertainty a conservative estimate is often used to determine the wind-induced response. For an isolated chimney excited by wind turbulence, the lower limit of the frequency provides a conservative prediction. For wake buffeting, on the other hand, the upper limit may have more serious effects. Therefore, it is recommended to analyse the structural effects for a sufficiently broad bandwidth of natural frequencies. © 1999 Academic Press

1. INTRODUCTION

The design of large reinforced concrete chimneys is usually based on the assumption of an isolated structure. In many power plants, however, considerable interference effects have to be expected, leading to higher or lower wind loads or wind load effects compared to the isolated structure. Clearly, a more severe loading will have to be considered in the design. It is less clear, whether advantage may be taken also of the shielding effect or whether the isolated structure should rather be considered as a minimum requirement for structural safety. For the sake of clarity, the building regulations in Germany follow the latter conservative principle. Interference effects are due to other high-rise buildings, for instance cooling towers or boiler houses. Additionally, two chimneys are often erected for a single unit to allow for a bypass operation in case that one chimney is under repair. The paper deals with the latter case, discussing for the example of two chimneys the wind-induced

0889–9746/99/100987 + 11 $30.00 © 1999 Academic Press

action and action effects in terms of base bending moments. The study is based on experiments in a boundary-layer wind tunnel. The characteristics of the modelled boundary-layer flow and the experimental set-up to measure the overall forces are described in Section 2. For a wide range of flow directions, the chimneys will behave similarly to an isolated chimney. The dynamic wind-induced action is mainly due to the turbulence of the oncoming flow. For other wind directions, however, vortices separating from the upwind chimney may hit the downwind chimney, thus inducing a further dynamic load. The basic differences between these two situations are considered in Section 3.

For the analysis of the action effects of the full-scale chimney, the mechanical admittance of the chimney has to be taken into account introducing an appropriate frequency and time scale. The basic relations are summarized in Section 4. The natural frequency of the chimney under design can only be estimated. Analytical methods and semi-empirical rules allow to predict the natural frequency, however with a remaining uncertainty, due for example to unclear foundation conditions. The sensitivity of the design wind load effect to a varying natural frequency is discussed in Section 5.

2. THE WIND TUNNEL EXPERIMENT

The wind tunnel experiments are performed in a boundary layer representing the typical characteristics of a wind flow over flat, open country. The boundary layer wind tunnel of the Ruhr-University Bochum is shown in Figure 1. It has a closed working section, 9·4 m long, 1·8 m wide and 1·6 m high with an adjustable ceiling, an open return, and a maximum flow speed of 30 m/s.

The boundary layer flow is generated using Counihan's (1969) method which has as special features, beside floor roughness, a set of turbulence generators and a castellated tripping bar to achieve an artificial thickening of the boundary layer. For a geometric scale of 1 : 500, the mean velocity profile and the corresponding turbulence intensity of the along-wind component are shown in Figure 2 and compared to the expected values in the atmospheric boundary layer using the ESDU (1986) model. Whilst the mean velocity flow obtained remains within the bandwidth of expected values for the full-scale flow in nature, the turbulence intensity shows slightly larger values in the wind tunnel experiment. This basically leads to turbulent wind loads which are slightly too high, i.e., the simulation is on the safe side.

The basic arrangement of the two 200 m high chimneys is shown in Figure 3. The clear distance between the two chimneys is chosen to be 3·25d, where d is the diameter of the chimney, which marks according to Zdravkovich (1988) the minimum distance for a side-by-side arrangement with no interference effects. Altogether, 10 test series have been

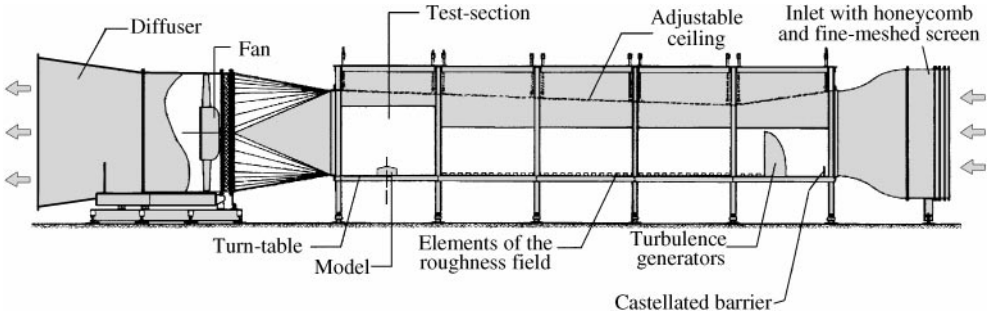

Figure 1. Boundary layer wind tunnel of the Ruhr-University Bochum.

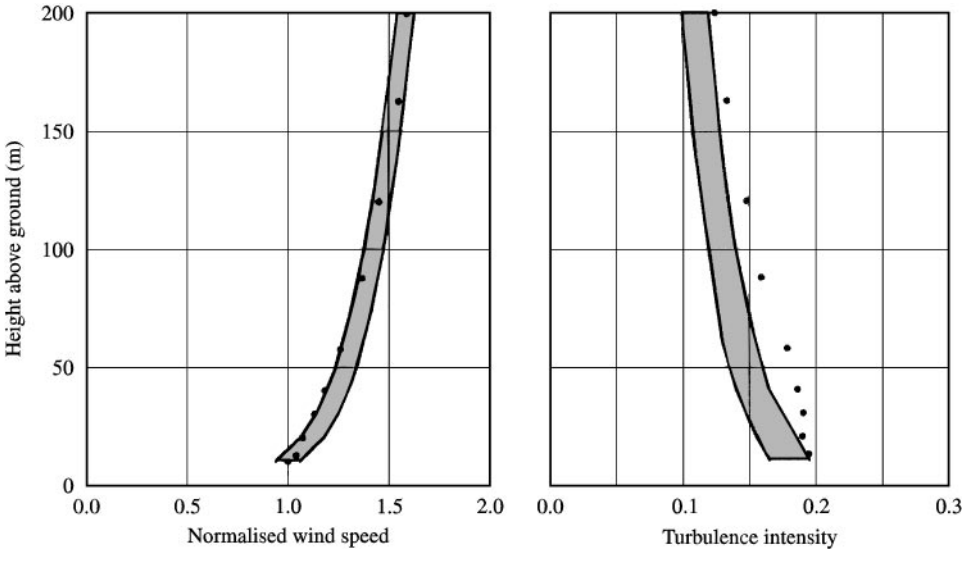

Figure 2. Comparison of the simulated boundary layer flow to the ESDU-model.

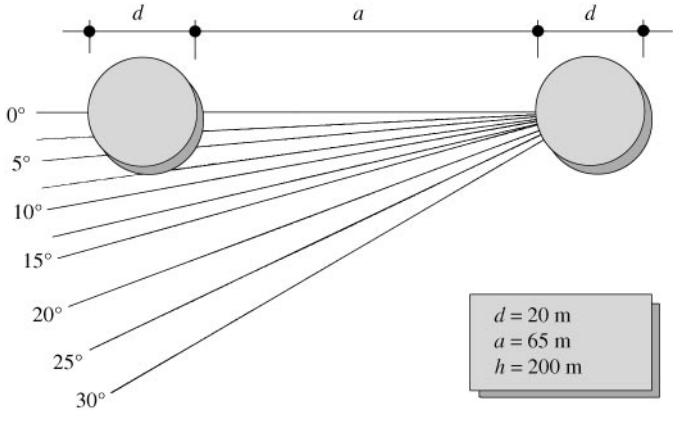

Figure 3. Basic test arrangement for the pair of chimneys.

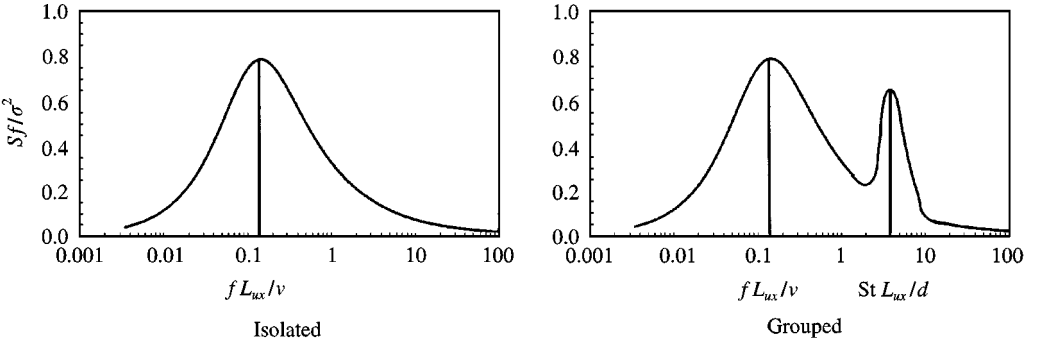

Figure 4. Base bending moment in the windward direction for isolated and grouped stacks.

performed, varying the flow direction from 0 to 30°, where 0° is defined for the two chimneys being in a tandem arrangement.

The wind-induced forces are measured by a force balance which provides the bending strains in two orthogonal directions at two different levels. Four responses are obtained in this manner: the along- and across-wind bending moment at the base, and the corresponding transverse forces. Since the force balance acts as a mechanical filter, the frequency content of the useful signals (the wind-induced overall forces) may be distorted significantly. For very low frequencies, the balance behaves statically and the variances of the wind-induced forces are translated to variances of the base-bending moments with a weighting factor of 1. For higher frequencies the weighting factor increases and reaches its maximum for an excitation frequency equal to the natural frequency of the force balance. Beyond this frequency, the admittance function decreases and approaches zero. Theoretically, this distortion can be corrected by dividing the measured spectral density of the response by the mechanical admittance function of the force balance. Practically, only distortions below and around the natural frequency of the force balance can be removed since the correction factor becomes high at frequency ratios beyond 1·5 or so; the error always included in the mechanical admittance is amplified at the same ratio. Furthermore, unavoidable noise becomes more and more important as the useful signal decreases at high frequencies, i.e.,

$$S_{\mathrm{me}}(f) = S_{\mathrm{use}}(f) \cdot V(f)^2 + S_{\mathrm{noise}}(f), \tag{1}$$

where S_{me} is the spectral density function of the measured signal, S_{use} the spectral density function of the useful signal, S_{noise} the spectral density function of noise, and $V(f)$ the mechanical amplification.

The amplification function of the mechanical system force-balance model is given as

$$V(f) = \frac{1}{[(1 - f^2/f_0^2)^2 + 4Df^2/f_0^2]^{1/2}}, \tag{2}$$

where f_0 is the natural frequency of the system force-balance model, equal to 106 Hz, and D is the critical damping ratio of the system force-balance model, equal to 0·012.

Strictly speaking, for the measuring system, more then one natural frequency has to be taken into account. A second vibration mode can be identified for a frequency of 165 Hz. However, the amplitudes of the corresponding modal forces are, smaller by a factor of 1000, than the contributions of the lowest natural frequency. Hence, this influence can be neglected.

For frequencies considerably above the natural frequency of the force balance, the weighting factor for the useful signal becomes zero, i.e., the pure noise is obtained as measured signal and the complete information of the useful signal is lost. Hence, the natural frequency of the force balance has to be sufficiently high to ensure an appropriate resolution in the interesting frequency range.

3. EVALUATION METHODS FOR EXTREME WIND-INDUCED ACTIONS EFFECTS

Wind-induced actions in an interference situation differ considerably from those induced for the isolated chimney and therefore may require different evaluation strategies. For the isolated chimney, the spectral density function of the overall load resembles the well-known mono-modal shape of the spectral density function of the velocity fluctuations. Then, the extreme action effect can be obtained in the usual manner based on an analysis in the

frequency domain, as follows:

$$M_{\max} = \bar{M} + g\sigma_M, \tag{3}$$

where $\bar{M}$ is the mean value of base bending moment, σ_M the root-mean square (r.m.s.) value of base bending moment, and g the peak factor.

The r.m.s. value of the reaction is the square root of the corresponding variance which is obtained by integrating the spectral density of the measured base-bending moment. The influence of the noise is reduced by setting an upper limit f_{ul} of the integral

$$\sigma_M = \left(\int_{f=0}^{f_{ul}} S_{\mathrm{me}}(f)/V(f)^2 \, \mathrm{d}f \right)^{1/2}. \tag{4}$$

For slender structures excited by the windward turbulence, it is usually appropriate to assume a narrow extreme value distribution of the peaks. Then, the mean extreme can be used to define the design wind load. The mean peak factor is obtained as follows:

$$g = \sqrt{2\ln(\nu T)} + \frac{\gamma}{\sqrt{2\ln(\nu T)}}, \tag{5}$$

where γ is the Euler constant (equal to 0·5772), ν the cycling rate $= \sigma_{\dot{M}}/(2\pi\sigma_M)$, $\sigma_{\dot{M}}$ the r.m.s. value of the derivative of M with respect to time: $\mathrm{d}M/\mathrm{d}t$.

Since the spectral density function of the base-bending moment shows a mono-modal behaviour with a maximum in the low- to mid-frequency range (Figure 4), the response will increase steadily with increasing velocity due an increasing resonant contribution.

Interference effects may change this comfortable behaviour in two aspects. Due to the two contributions of along-wind turbulence and wake-buffeting, the spectral density function shows two relative maxima (Figure 4). Then, the wind load effect will first increase with velocity until full resonance with the wake buffeting is obtained. Beyond that point, the wind load effect will decrease with further increasing wind speed, until resonance due to along-wind turbulence will start to govern the dynamic response. For further increasing wind speeds the wind load effect will again increase steadily.

As a further difference, it has to be noted that it is no longer clear if the extreme value distribution is narrow enough to justify that the mean extreme may be used to define the design wind load. For a considerable coefficient of variation of the extremes, Cook & Mayne (1980) recommended to use the 78% fractile of the extremes instead of their mean value. For the extreme value distribution, a Gumbel distribution is assumed as follows:

$$p(M \le M_{\max}) = \exp\left\{ -\exp\left[-\left(\gamma + \frac{\pi}{\sqrt{6}} \frac{M_{\max} - \overline{M_{\max}}}{\sigma_{M_{\max}}} \right) \right] \right\}, \tag{6}$$

where $\overline{M_{\max}}$ is the mean value of the extreme base-bending moment, and $\sigma_{\mathrm{M}_{\max}}$ the r.m.s. value of the extreme base-bending moment; the coefficient of variation is defined as the ratio of the r.m.s. to the mean value of the extremes:

$$\text{coefficient of variation: } \sigma_{M_{\max}}/\overline{M_{\max}}. \tag{7}$$

Setting for the probability a value of $p = 0{\cdot}78$ then leads to the following expression for the 78% fractile:

$$M_{\max,78\%} = \overline{M_{\max}} + 0{\cdot}636\sigma_{M_{\max}}, \tag{8}$$

where $M_{\max,78\%}$ is the 78%-fractile of the extreme base bending moment.

If the coefficient of variation is not small (say larger than 10%), a further point of complication lies in the consideration of the appropriate time scale. Equation (8) defines the 78%-fractile for the time window used in the wind tunnel experiment. The corresponding period of time in full scale is obtained from the time scale taking into account the geometric scale and the velocity scale as follows:

$$\lambda_T = \frac{\lambda_L}{\lambda_v} \tag{9}$$

with the basic definition of a scale λ for a variable x:

$$\lambda_x = \frac{x_{\text{wind tunnel}}}{x_{\text{full-scale}}}. \tag{10}$$

For different wind velocity levels in full-scale, the actual duration T_{act} will change and may differ considerably from the intended duration T_{ref} which for example is 1 h. Hence, the mismatch of T_{act} and T_{ref} for certain velocity levels has to be taken into account, too. If the actual duration is smaller than the time window T_{ref}, the 78%-fractile obtained from the pure wind tunnel results is too small; if, however, the actual duration is larger, the estimated fractile is too large. Assuming again the Gumbel distribution for the extreme value distribution of $M_{\max}$ leads to the following relation to estimate the appropriate fractile value:

$$M^*_{\max,78\%} = \frac{\sqrt{6}\sigma_{M_{\max}}\{-\ln[-\ln(0{\cdot}78T_{\text{act}}/T_{\text{ref}})]-\gamma\}}{\pi} + \overline{M_{\max}}. \tag{11}$$

For T_{act} equal to T_{ref}, equation (8) is obtained.

The evaluation of the mean extreme and the corresponding r.m.s. value requires an analysis in the time domain. The basic strategy, therefore, includes the following steps: (i) transformation of the time signal via Fast Fourier Transformation (FFT) into the frequency domain; (ii) correction of the influence of the mechanical admittance of the force balance; (iii) weighting of the signal with the mechanical admittance of the full-scale building taking into account the appropriate frequency scale; (iv) re-transformation of the signal into the time domain via an Inverse Fast Fourier Transformation (IFFT); (v) sampling of the extreme base-bending moment.

The appropriate frequency scale is obtained as the inverse of the time scale in equation (9). The mechanical admittance is a complex function and is given for a single-degree-of-freedom system as follows:

$$H(\mathrm{i}\omega) = \frac{\omega_0^2 - \omega^2 - \mathrm{i}2D\omega_0\omega}{(\omega_0^2-\omega^2)^2 + 4D^2\omega_0^2\omega^2}\,\frac{1}{m}, \tag{12}$$

where $\omega = 2\pi f$, $\omega_0 = 2\pi f_0$, f is the excitation frequency, f_0 the natural frequency, D the critical damping ratio, and m the modal mass.

To obtain a sufficiently high statistical stability for the estimations of the mean and r.m.s. value of the extremes, a sufficiently large number N of independent runs is needed. In Kasperski *et al.* (1996) confidence intervals are shown for the mean extreme and the corresponding r.m.s. value using a reduced variate which originally follows a Gumbel distribution. Based on these results, $N = 60$ has been chosen for the present study.

4. ESTIMATION OF THE NATURAL FREQUENCY

During the design process, the natural frequency of the chimney has to be estimated by simplified analytical or semi-empirical or empirical formulae. According to Eurocode 1, the

fundamental flexural frequency f_0 of a chimney of constant diameter and constant mass and stiffness distribution can be estimated as follows:

$$f_0 = \frac{\varepsilon d}{h^2}\sqrt{\frac{W_s}{W_t}}\,[\mathrm{Hz}], \tag{13}$$

where d is the diameter of the chimney (m), h the height of the chimney (m), ε a constant taking into account the material properties with values of 1000 for steel chimneys, 700 for reinforced concrete or masonry chimneys. W_s is the weight of structural parts contributing to the stiffness of the chimney, and W_t the total weight of the chimney.

For the present study, the liner weight is assumed to be 35% of the weight of the shaft. Then, equation (13) leads to an estimated natural frequency of 0·30 Hz. Usually, mass and stiffness are not uniformly distributed. This can be taken into account for example by an appropriate finite element analysis. Additionally, the actual soil conditions may have a considerable influence on the lowest natural frequency. In the easiest model, the soil stiffness is taken into account by a linear spring at the base. Clearly, uncertainties in the estimation of the soil parameters lead to uncertainties in the estimated natural frequency. For the present study, therefore, a bandwidth of the lowest natural frequency from 0·20 to 0·30 Hz is assumed.

For a mono-modal excitation typically caused by the along-wind turbulence, the worst load effect generally is obtained for the lowest natural frequency. Resonant excitation due to wake-buffeting, on the other hand, is worse for a higher frequency since the inertia forces increase with increasing frequency. Hence, a careful analysis for a wider range of frequencies becomes necessary.

5. RESULTS AND DISCUSSION

As a first step, the wind-induced actions are analysed in terms of the global overturning moment. The 60 time series for each of the 10 test series (corresponding to 10 flow directions) therefore are corrected only with the mechanical admittance of the force balance. As basic statistical parameters, the mean value, the r.m.s. value and the mean extreme value are calculated. The results are shown in Figure 5. Clearly, the largest interference effect is obtained for a flow direction of 15°.

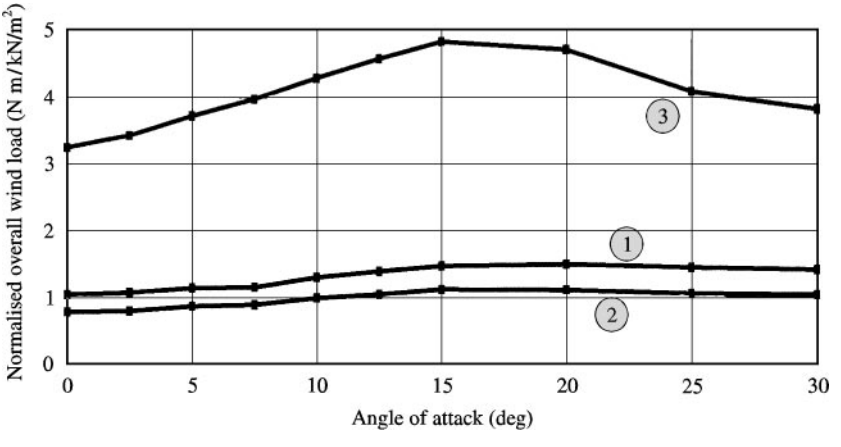

Figure 5. Mean value, r.m.s. value of the parent distribution and mean of the extremes of the overturning moment [all results in (Nm/kN/m^2); original wind tunnel data]. (1): mean value; (2) r.m.s. value; (3) mean extreme.

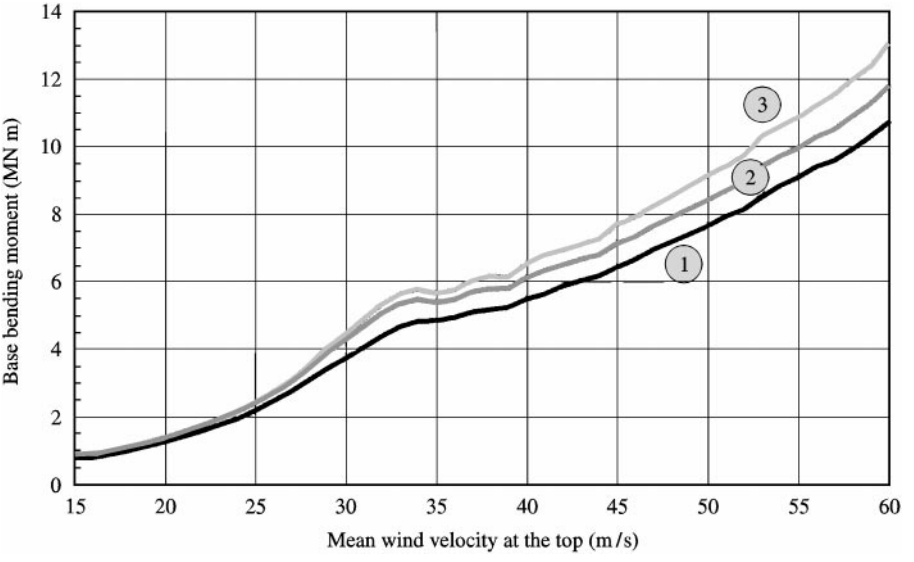

Figure 6. Base bending moment for the chimney with a natural frequency of 0·3 Hz. Comparison of the mean of the extremes with the 78%-fractile obtained directly from the wind tunnel results and the appropriate 78%-fractile using the correct time scale. — (1) mean of the extremes; — (2) 78%-fractile without correction for time scale; — (3) 78%-fractile with correction for time scale.

TABLE 1

Base bending moment for the chimney with a natural frequency of 0·3 Hz. Comparison of the mean extreme value to the pure 78%-fractile from the wind tunnel and the appropriate 78%-fractile using the correct time scale

Mean wind speed at the top (m/s)	Mean of the extremes (MN m)	78%-fractile without correction for the time scale (MN m)	78%-fractile with correction for the time scale (MN m)
15	0·80	0·88	0·84
20	1·26	1·39	1·36
25	2·19	2·42	2·44
30	3·75	4·31	4·47
35	4·87	5·41	5·68
40	5·51	6·13	6·54
45	6·43	7·15	7·71
50	7·66	8·44	9·16
55	9·11	9·98	10·88
60	10·74	11·83	13·08

The next question deals with the influence of the coefficient of variation of the extremes on the design wind load. Hence, the mean extreme wind action effect is compared to the appropriate 78%-fractile. To show the influence of the time window, as intermediate step the 78%-fractile of the pure wind tunnel results (i.e., the 78%-fractile without time scale) is given. The analysis is performed on the example of a structure with a natural frequency of 0·3 Hz. The results are plotted versus the mean wind speed at the top of the chimney in Figure 6. Additionally, the results are summarized in Table 1.

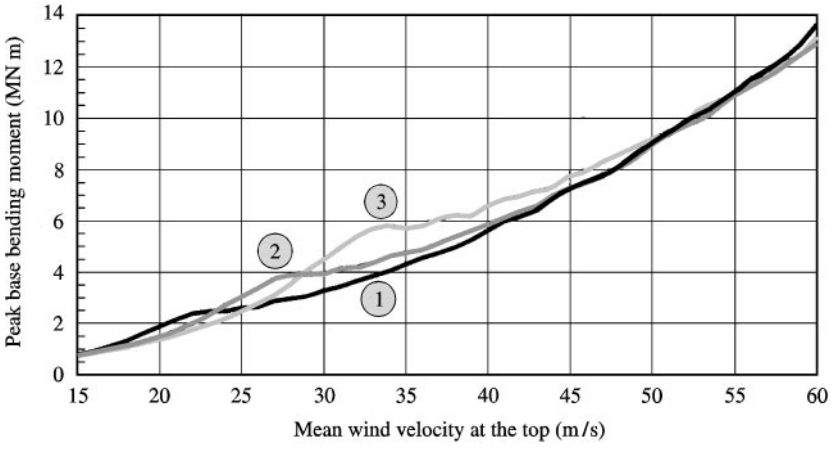

Figure 7. Extreme base bending moment for three different natural frequencies assuming worst interference. Natural frequency — (1): 0·2·Hz; — (2) 0·25 Hz; — (3): 0·30 Hz.

The appropriate 78%-fractile turns out to be approximately 20% larger than the mean of the extremes. Hence, for the design it is strongly recommended to use this value. The influence of the coefficient of variation of the extremes can be seen by comparing the uncorrected 78%-fractile to the mean extreme. Obviously, this ratio varies over the range of wind speeds. Values between 1·1 and 1·15 are obtained. The maximum is reached for full resonance with the peak of wake buffeting at a wind speed of 33 m/s. The corresponding coefficient of variation is about 23% while, for the other wind speed levels governed mainly by resonance with the along-wind turbulence, the coefficient of variation is 15%. The influence of the correct time window changes over the wind speed. For low wind speeds, the difference between the mean of the extremes and the 78%-fractile with correction for time scale remains small due to the fact that the time window used in the wind tunnel experiments is too long. For wind speeds above 25 m/s, the time window becomes too short, hence the difference between the mean of the extremes and the corrected 78%-fractile increases. A relative maximum is obtained for that wind speed where full resonance with the wake buffeting occurs.

For the present study, a reference wind speed of 45 m/s has been chosen. This wind speed is exceeded in each year with a probability of $p = 0{\cdot}02$. The design wind speed is defined as that wind speed which is exceeded with a probability of $p = 0{\cdot}05$ in the projected lifetime of the structure, which here is assumed to be 50 years. Assuming a Gumbel distribution for the extreme wind speeds and introducing for the coefficient of variation a value of 12.5% which corresponds to the typical wind climate in Europe induced by winter storms, a design wind speed of 54 m/s is obtained.

Figure 7 shows the base-bending moments for three different natural frequencies. As has to be expected, all curves show a relative maximum due to resonance with the turbulence induced by wake buffeting. The corresponding wind speeds increase with the natural frequency of the chimney. The worst effect is obtained for the highest natural frequency.

Theoretically, for very large wind speeds, the largest wind-induced action effect should occur for the lowest natural frequency. However, the results obtained do not clearly show that expected trend. Especially, the curves for $f_0 = 0{\cdot}25$ and $0{\cdot}30$ Hz show a kind of criss-cross behaviour which indicates that remaining scatter due to statistical uncertainties is still influencing the results. For clearer results, therefore, the number of independent experiments has to be increased further to, for example, 200 or even more experiments.

The design situation for the extreme wind speed of 54 m/s surprisingly shows no considerable difference between the three estimated values of the natural frequencies. Taking the worst value, the design base-bending moment becomes 10·5 MN m. Taking into account the usual safety factor of $\gamma = 1{\cdot}75$ for reinforced concrete, the level of wind load effect can be calculated where first cracks should occur. For the above example, this value becomes 6 MN m. This limit is approached or crossed at different levels of wind speed. For the two lower natural frequencies 0·20 and 0·25 Hz, first cracks are likely to occur for a wind speed of approximately 40 m/s. This wind speed is exceeded in a single year with a probability of 0·088. For a natural frequency of 0·3 Hz, first cracks are predicted for a wind speed of 37 m/s. This wind speed level is exceeded with a probability of 20% in a single year. The probability of obtaining cracks increases with each year of working life. The basic relation is as follows:

$$p_N(v > v^*) = 1 - (1 - p(v \leq v^*))^N, \tag{14}$$

where $p_N(v > v^*)$ is the exceedence probability in N years, and $p(v \leq v^*)$ the nonexceedence probability in a single year.

It can be used for further analysis with regard to serviceability and durability of the structure. For the two lower natural frequencies ($f_0 = 0{\cdot}2$ and 0·25 Hz), a 50% probability of obtaining cracks is accumulated within 7–8 years. The situation becomes even worse for the upper bound of estimated natural frequencies. For a natural frequency of 0·3 Hz, the structure will withstand the wind-induced forces without getting cracks for a period of only 3 years with a probability of 50%. Clearly, these results have to be taken into account in design considerations. The situation can be improved by considerably increasing the design-bending moment or the design wind speed, respectively. For a design wind speed of 60 m/s, the probability of obtaining cracks in the first 10 years is reduced to 20% for a natural frequency of 0·3 Hz and to 8% for natural frequencies between 0·2 and 0·25 Hz.

For the sake of discussion, the highest estimate of the natural frequency may be interpreted as the true natural frequency of the uncracked shaft. As cracks develop, the natural frequency drops gradually to values, say, of 0·25 and 0·20 Hz. The wind-induced base bending moments for these situations are plotted in Figure 7 as a function of the mean wind speed. It can be seen that the effect of wake buffeting is largest for the uncracked shaft. It becomes less and less important as the stiffness decreases due to cracking. Therefore, the structural response is strongest at the beginning of the lifetime over a wide range of wind speeds. However, as the natural frequency drops with increasing structural life, the response is diminished. In other words, a self-healing effect is caused by a decrease of the structural stiffness in the case of a bimodal excitation.

6. CONCLUSIONS

This study on interference effects between two 200 m high reinforced concrete chimneys leads to the following main conclusions.

(i) Interference leads to a mixed excitation mechanism. Besides resonance due to turbulence in the oncoming flow, considerable resonance due to wake buffeting may occur. While for the first mechanism the worst situation is obtained for the lowest estimated natural frequency, the second mechanism becomes strongest for the upper estimated value. Hence, the analysis should include a wider band of estimated lowest natural frequencies. Depending on the actual wind climate, the upper limit of the estimated natural frequency may become dominant for the design.

(ii) For interference situations, the coefficient of variation of the extreme wind-induced action effects cannot be assumed to be small. Hence, an appropriate fractile of the extreme action effects should be used to define the design wind load. As a first step, it is recommended to use the 78%-fractile as proposed by Cook and Mayne (1980).

(iii) The ultimate limit state is governed clearly by resonant vibrations due to the along-wind turbulence. Surprisingly, the design wind loads show only a small sensitivity with regard to a wrong estimate of the natural frequency. Resonance due to wake buffeting on the other hand has to be taken into account in regard to serviceability and durability aspects. The probability of obtaining cracks strongly depends on the lowest natural frequency of the structure. If the natural frequency is estimated with too small a value, an underdesign may arise in terms of serviceability and durability.

(iv) Depending on the initial value of the lowest natural frequency of the structure just after the erection phase, the structural behaviour may vary considerably over the lifetime. In case of a relatively large initial value, a kind of self-healing effect may be expected, i.e., cracks may lead to a more favourable structural behaviour. To include these effects in the design of the structure, adequate strategies have to be developed to take into account the unequally distributed accumulation of the overloading risk over the lifetime of the structure.

The study so far has not taken into account the influence of a wind climate with considerable directional effects. For example, in Germany the strongest winds have to be expected from southerly to westerly wind directions, while easterly wind directions are characterized by a relatively weaker wind climate. Depending on the orientation of the stacks, interference might become less important if, for example, the strongest interference direction corresponds to the weaker wind directions.

References

COOK, N. J. & MAYNE, J. R. 1980 A refined working approach to the assessment of wind loads for equivalent static design. *Journal of Wind Engineering and Industrial Aerodynamics* **6,** 125–137.

COUNIHAN, C. 1969 An improved method of simulating an atmospheric boundary layer in a wind tunnel. *Atmospheric Environment* **3,** 197–214.

ESDU—Engineering Science Data Unit 1986 Characteristics of atmospheric turbulence near the ground. Single point data for strong winds. ITEM 86010.

KASPERSKI, M., KOSS, H. and SAHLMEN, J. 1996 BEATRICE joint project: wind action on low-rise buildings. Part 1. Basic information and first results. *Journal of Wind Engineering and Industrial Aerodynamics* **64,** 101–125.

ZDRAVKOVICH, M. M. 1988 Review of interference-induced oscillations in flow past two parallel circular cylinders in various arrangements. *Journal of Wind Engineering and Industrial Aerodynamics* **28,** 183–200.